GEOPHYSICS, VOL. 73, NO. 6 (NOVEMBER-DECEMBER 2008); P. WA83–WA93, 10 FIGS.
10.1190/1.2992507

Monitoring aquifer recharge using repeated high-precision gravity measurements: A pilot study in South Weber, Utah

D. S. Chapman[1], E. Sahm[1], and P. Gettings[1]

ABSTRACT

Repeated high-precision gravity surveys were conducted over two infiltration cycles on an alluvial-fan aquifer system at the mouth of Weber Canyon in northern Utah as part of the Weber River Basin Aquifer Storage and Recovery Pilot Project (WRBASR). Gravity measurements collected before, during, and after infiltration events indicate that a perched groundwater mound formed during infiltration events and decayed smoothly following infiltration. Data also suggest the groundwater mound migrated gradually south-southwest from the surface infiltration site. Maximum measured gravity changes associated with the infiltration were 111 μGal during the first event (2004) and a net 130-μGal increase during the second event (2005). Gaussian integration of the spatial gravity anomaly yields an anomalous-causative mass within 10% of the 10^6 m^3 (10^9 kg) of infiltrated water measured in 2004. The spatial gravity field is consistent with a groundwater mound at the end of the infiltration cycle approximately equivalent to a cylindrical disc of height 13.5 m and a radius between 300–400 m. After infiltration ceased, gravity anomalies decreased to approximately 50% of their original amplitude over a characteristic time of three to four months. The reduction of the gravity signal is simulated by analytical solutions for the decay of a groundwater mound through a saturated porous media. This comparison places relatively tight bounds on the hydraulic conductivity of the alluvial-fan material below the infiltration site with a preferred value of 80 m/day on a length scale of a few hundred meters.

INTRODUCTION

Declining groundwater levels and water quality resulting from increasing use and expanding water budgets is a growing problem in Utah and much of the western United States (Stonely, 2004; Hurlow et al., 2008). Consequently, aquifer recharge has become an increasingly popular method for water storage and aquifer conservation in many drought-prone areas (Clyde et al., 1984; Pyne, 1995; Hurlow et al., 2008). One challenge of aquifer recharge and storage monitoring is finding a cost-efficient, effective way to monitor subsurface water transport to determine if infiltrated water remains in target areas.

Previous studies show that repeated high-precision gravity measurements are capable of detecting gravity changes associated with injecting or withdrawing fluids from subsurface reservoirs, e.g., Allis and Hunt, 1986; Pool and Eychaner, 1995; Keysers et al., 2001; Ferguson et al., 2007. This paper presents a case study in which repeated gravity surveys were taken during the Weber River Basin Aquifer Storage and Recovery Pilot Project (WRBASR), conducted at the mouth of Weber Canyon in northern Utah between February 2004 and August 2005.

Detailed analysis of the gravity survey data was conducted to determine the accuracy, reliability and sensitivity of high-precision gravity measurements as a reliable means to monitor aquifer recharge. Gravity data collected before, during, and after infiltration events were analyzed to track groundwater movement during the study. The data indicate that a significant gravity anomaly formed during each infiltration event. The anomaly broadened over time, indicating south-southwest groundwater flow from the infiltration site. Analysis of spatial gravity anomalies provides a quantitative comparison of the mass calculated from measured gravity anomalies to the known infiltrated mass and also provides constraints on the geometry of the groundwater mound formed under the infiltration ponds. We compare the decrease of the gravity anomaly after infiltration ceased to the diffusive decay of a groundwater mound in a saturated porous media. Ultimately, this comparison helps set a range of probable formation scale (100 m scale) hydraulic conductivities of the alluvial fan and aquifer system.

Manuscript received by the Editor 29 February 2008; revised manuscript received 30 June 2008; published online 20 November 2008.
[1]The University of Utah, Salt Lake City, Utah, U. S. A. E-mail: david.chapman@utah.edu; sahm@earth.utah.edu; gettings@earth.utah.edu.

PROJECT AND SITE DESCRIPTION

The WRBASR project was a three-year, multiagency cooperative effort to evaluate the feasibility of artificial aquifer recharge in the Weber Delta area of northern Utah (Lowe et al., 2003). Infiltration ponds are located 1.6 km west of the mouth of Weber Canyon, where the Weber River flows from the Wasatch Range across the Weber River Delta (Figure 1). The delta was formed as the Weber River flowed into Pleistocene-aged Lake Bonneville. The Weber River Delta contains two principal aquifers: the shallower Sunset and deeper Delta aquifers (Figure 2) with a combined thickness of about 300 m. Tertiary basin fill below these aquifers is typically more lithified and less permeable. Both aquifers are composed of interbedded sand and gravel deposits, with lenses of low-permeability clay and silty clay. The infiltration ponds are in the easternmost unconfined part of the alluvial-fan system where the Sunset and Delta aquifers cannot be distinguished (Hurlow et al., 2008).

The nature of the groundwater system within the Weber River Delta deposits is summarized in Hurlow et al. (2008); detailed discussions are found in Feth et al. (1966), Clark et al. (1990), Anderson et al. (1994), and Gates (1995). The aquifers are recharged primarily by infiltration from the Weber River and from bedrock flow out of the Wasatch Mountains. Recharge to the Weber aquifer systems is estimated to be between 0.08–0.13 km^3/yr, partitioned between river and stream seepage (33%), canal and irrigation seepage (7%), precipitation (11%), and subsurface flow from the Wasatch Mountains (49%). The Weber River loses water to the unconsolidated aquifers for a distance of 2.4 km after it emerges from Weber Canyon; infiltration over this section varies from 3% of the Weber River flow during flood to 20% during low flow.

Groundwater flow in the aquifer system is generally from the recharge zone near the Wasatch Range westward to the Great Salt Lake; horizontal hydraulic gradients vary from 1–2 m/km. Water levels in eight wells within 6 km of the infiltration site were compiled (Hurlow et al., 2008) to determine the seasonal fluctuations in the water table and any longer term trends. Most of the wells show from 1–10 m of drawdown in response to summer pumping and 1–3 m seasonal change. Water levels in the unconfined aquifer have declined by about 26 m since 1953, reflecting the increase in groundwater withdrawal in the area from 12 million cubic meters in the 1950s to 43 million cubic meters today. Annual precipitation in the region is 50 cm/yr, considerably less than the potential evapotranspiration of 114 cm/yr (Hurlow et al., 2008).

The WRBASR project site consists of 36,000 m^2 (nine acres) of land immediately west of an active sand and gravel quarry. The property is bounded on the north by an irrigation canal that allows water to be diverted from the Weber River for infiltration. The upper few meters of gravel-rich deposits were removed during construction of the infiltration ponds, exposing interbedded sand and gravel. Four infiltration ponds were constructed, totaling ~15,000 m^2 of surface area (Figure 3). The smallest of the basins received the diverted water first and functioned as a sedimentation basin to remove fine-grained and suspended material from the water.

One monitoring well was installed at the west end of the project site (Figure 2) to monitor changes in water levels. The well is 92 m deep and is screened below 82 m; the depth to the water table is about 70 m. The well encountered a silty layer from 35–39 m depth, above the water table but within the unconfined aquifer (Hurlow et al., 2008). The top 0.5 m of this layer is especially clay rich. This silty layer is visible in the gravel pit 400 m to the east of the infiltration site, where it crops out at an elevation 5 m lower than in the monitoring well. In addition, the silty layer is mentioned in logs of installed wells elsewhere in the area, suggesting extensive lateral continuity (Hurlow et al., 2008). It is likely that this low-permeability layer created a shallow, perched water mound from the infiltrated water (Figure 2). Infiltration was interrupted in both 2004 and 2005 when seepage occurred in the easterly gravel pit at the top of the silty layer.

A high-precision gravity study was conducted to track infiltrated groundwater movement in lieu of installing multiple groundwater monitoring wells (Hurlow et al., 2008; Lowe et al., 2003). This technique has many advantages in addition to the financial savings of avoiding monitoring wells. Gravity measurements represent a direct measurement of the accumulated mass of infiltrated water, although changes in water level of monitoring wells resulting from infiltration could

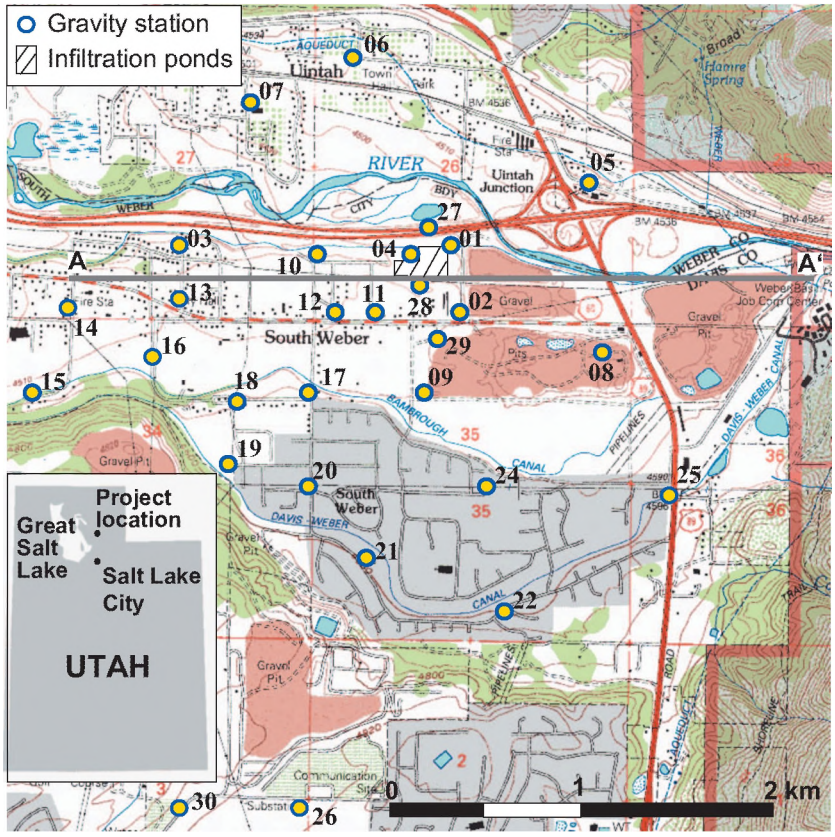

Figure 1. Location of the Weber River Basin Aquifer Storage and Recovery Project (WRBASR) in northern Utah (inset). Base map includes the Wasatch Mountains to the east and the Weber River flowing out of the Wasatch Mountains across the Weber Delta alluvial fan. Open circles represent gravity-monitoring stations; the prefix *WRP* on station numbers has been omitted to avoid clutter. Infiltration ponds (cross hachure) are near station 04. The west-east cross section A – A′ appears in Figure 2.

be delayed. Gravity surveys also offer the possibility of tracking subsurface mass spatially as infiltration proceeds.

Two annual infiltration events were conducted in the late spring through summer of 2004 and 2005. The four passive infiltration ponds were flooded with water diverted from the Weber River from 19 March to 2 July 2004, and between 17 March and 31 October 2005. Infiltration was suspended on 2 July 2004, and again between 24 May and 16 August 2005, because of seepage into an adjacent gravel pit (Hurlow et al., 2008).

Prior to infiltration, a grid of 30 gravity stations surrounding the infiltration ponds was established (Figure 1). Four stations (WRP01, WRP04, WRP27, and WRP28) were placed within 100 m surrounding the infiltration ponds. Station density decreases away from the project site. More stations were placed to the south and west of the site, because the infiltrated water was expected to flow in these directions based on regional dip of layers making up the Sunset and Delta aquifers and the regional hydraulic gradient. Three of these stations (WRP26, WRP30, and WKRP) were located several kilometers from the infiltration site to monitor region-scale, seasonal fluctuations in the gravity signal during the infiltration events. High-precision gravity surveys require stable, level platforms for the gravimeter and global-positioning system (GPS) equipment. Where possible, gravity stations were established on existing cement pads to reduce cost and environmental impact. Three stations (WRP01, WRP27, and WRP28) were installed in bare ground by cementing a 31-cm paving stone around a 1.2-m rebar rod driven to ground level (Hurlow et al., 2008). During the course of the study, some sites were abandoned because of accessibility issues (WRP03) or because little or no observed change in gravity was observed (WRP14, WRP15). Station WRP23 was never developed and is not shown on Figure 1. A far-field control site, WRP26, was destroyed by construction in the fall of 2004 and was replaced with WRP30, located approximately 600 m southwest of WRP26 (Hurlow et al., 2008). WRP27, WRP28, and WRP29 were not added until June 2004.

FIELD MEASUREMENTS

Gravity survey methods

Gravity surveys were conducted before, during and after recharge events to capture the pre-infiltration background, growth, peak, and subsequent decrease of the gravity signal. During both infiltration events, we made gravity surveys approximately every two weeks. After infiltration ceased, surveys continued every three to four weeks through October in 2004 and mid-August in 2005. We also conducted GPS surveys approximately every six weeks to monitor any elevation change at each site throughout the project.

Multiple techniques are available for high-precision gravity surveying and analysis (Whitcomb et al. 1980; Dragert et al., 1981; Jachens et al., 1981; Gettings, 2005; Ferguson et al., 2007; Gettings et al., 2008). The WRB ASR pilot project used the technique presented in Gettings (2005) and Gettings et al. (2008), which combines an automated gravimeter and rapid-static differential GPS measurements. Gravity measurements were collected using a Scintrex CG-3M automated gravimeter, which statistically averages time-series gravity data collected at each station. Scintrex reports the precision of the CG-3M gravimeter used in this study to be 1 μGal; previous field studies have found detection limits of 10 μGal (Budetta and Carbone, 1997; Bonvalot et al., 1998). Analysis of instrument drift, environmental noise, and measurement repeatability suggest an accuracy of ±5 μGal in our study. A gravity change of 10 μGal would be detected unambiguously, avoiding overlapping error bars in the measurements.

Major challenges in high-precision gravity observations include accounting for drift and random variation of the measurements. Our gravity surveys were divided into multiple station loops consisting of five to seven stations, with the first and last occupation of each loop returning to a designated "base" station (typically WRP12). During each survey, every station loop was occupied twice, so that each station had at least two measurements per campaign to aid in monitoring nonlinear instrument drift (Gettings, 2005). Each occupation involved a 12- to 15-minute continual measurement of gravi-

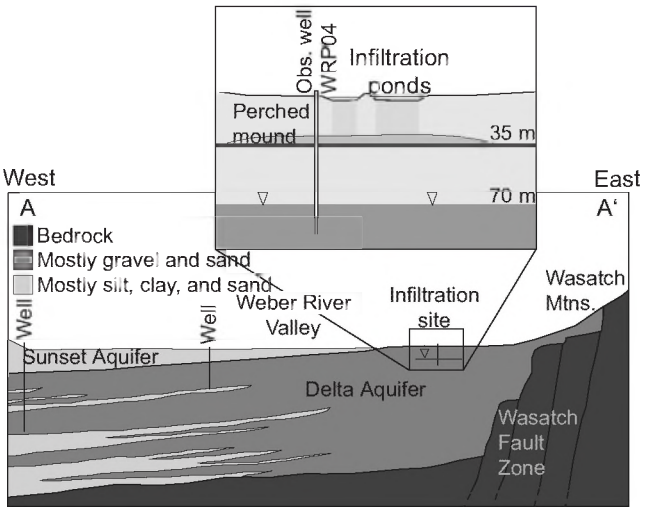

Figure 2. Generalized cross section of Weber River Basin alluvial fan deposited west of the Wasatch Mountains and the Wasatch Fault Zone. The alluvial fan is composed of sands and gravels in two identified aquifers. The expanded section shows schematic details of the infiltration site including infiltration ponds, a perched water mound on a silty layer 35 m below the surface, and water table at 70 m. Modified from Lowe et al. (2003).

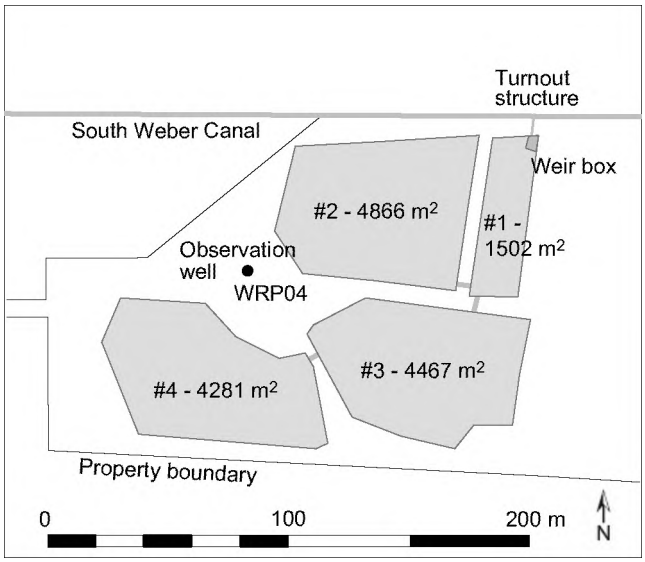

Figure 3. Infiltration-pond layout with locations of the monitoring/observation well and gravity station WRP04.

ty over which a time-series average was computed. The 15-minute occupation allows for decay of transient transport effects (3–5 minutes) and for sufficient data collection to average out small-scale, random noise. To monitor long-term instrument drift between survey campaigns, continual measurements were taken on a seismic pier in room 115 of the William Browning Building at the University of Utah in Salt Lake City, UT. These techniques assume that same-day changes in actual gravity are zero (after tidal correction), and that changes in gravity readings on the same day at a given site represent instrument drift.

Details of the techniques used for reduction of the raw gravity data are described in Gettings (2005) and summarized here. The CG-3M gravimeter automatically corrects for instrument tilt during data acquisition (via two internal tilt meters) and deviations in internal temperature from 55°C. A harmonic earth-tide correction is made following the procedure of Tamura (1987). The first three minutes of data are removed to avoid transient transport effects, and the remaining time-series data are reduced to a single value using a weighted average of the readings. Repeated station occupations (within four to five hours of each other) quantify the nonlinear drift, which is removed during processing. The gravimeter is set to track linear drift over time. This linear drift constant is adjusted as gravity data from the base station at the University of Utah are collected. Consideration of survey measurement error caused by vibrations from vehicle/pedestrian traffic, wind, instrument drift, corrections accounting for earth tides, and repeatability tests suggest that measured field values are accurate to within ±5 μGal of actual values. Considering that expected peak-gravity anomalies from infiltration were anticipated to exceed 100 μGal based on the planned infiltration volume, the gravity surveys were able to distinguish the actual infiltrated-water gravity signal from instrument drift and error.

We began gravity measurements one month before infiltration to establish background levels and natural signal (Hurlow et al., 2008). After infiltration began, we computed gravity changes over time for each site by comparing measurements from each campaign to the average of the pre-infiltration campaigns (prior to 19 March 2004). To enhance the infiltration signal, we subtracted the average change in gravity observed at stations WRP16, WRP18-22, WRP26, and WRP30 from all stations in each survey. These far-field reference stations are sufficiently removed from the project site (a lateral distance of at least 1 km) to justify an assumption that no local infiltration volume affects them. Few of these sites showed any systematic gravity change during infiltration, and none beyond an assumed natural variability/noise of 10 μGal.

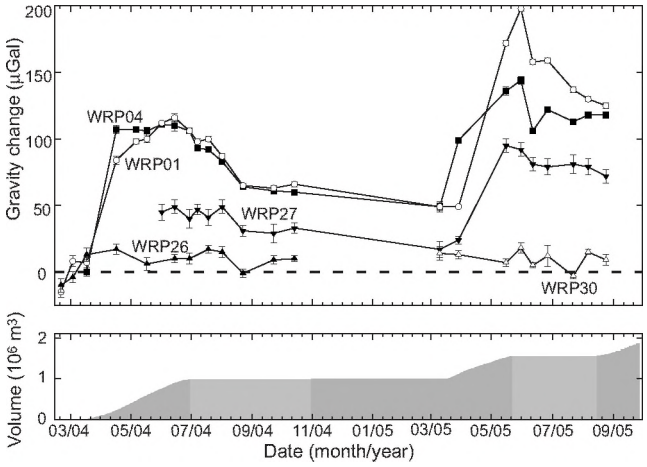

Figure 4. Gravity monitoring in relation to aquifer recharge. The lower section shows cumulative water-infiltration volume in two recharge cycles, spring 2004 and spring-summer 2005. The upper section shows gravity changes observed at three sites near the infiltration ponds (WRP04, WRP01, and WRP27) and two far-field sites that show the nature of the background gravity field unaffected by artificial recharge (WRP26 and WRP30).

Gravity-monitoring results

Figure 4 shows the volume of water recharged into the aquifer combined with the variation in gravity at selected stations representing stations nearest the infiltration pond (WRP04 and WRP01), within 500 m of the ponds (WRP27), and regional control stations (WRP26 and WRP30). By 2 July 2004, approximately 1,000,000 m^3 of water (10^9 kg) had infiltrated into the aquifer. Gravity at station WRP04, closest to the infiltration site, increased by about 110 μGals after 30 days of infiltration, remained fairly steady, and then increased again slightly to reach a maximum at the end of infiltration on 1 July. Station WRP04 is immediately adjacent to and down-hydraulic gradient from the infiltration ponds (Hurlow et al., 2008). It showed the earliest and largest gravity signal in 2004. It was surprising to see station WRP04 reach most of its eventual amplitude long before the full volume of the first infiltration event was attained. Because WRP04 is at the edge of the infiltration ponds (Figure 3), this rapid gravity response must be caused by the added mass accompanying saturation of the vadose zone below the ponds and above the silty layer. Approximating the vadose-zone saturation below the ponds as vertical cylinders yields a gravitational attraction of about 90 μGal at WRP04, the correct order of magnitude for the observed change. We also considered the possibility that readings at WROP04 are affected by water in the infiltration ponds kept at a depth of 0.5–1.0 m. However, the station is at an elevation close to the bottom of the ponds and therefore the gravitational attraction by pond water would be predominantly horizontal.

Station WRP01 is also close to the site, but upgradient from the ponds. It also would be affected by vadose-zone saturation during infiltration, but with a slightly reduced and delayed response compared to WRP04 because of the station location. The 2004 gravity anomaly at WRP01 peaks at the end of the infiltration event. Station WRP27 is farther from the site than WRP01 and is also up-hydraulic gradient; it shows an even more reduced and delayed signal. In general, the gravity signal is delayed in time and reduced in amplitude as one moves away from the infiltration site.

Regional control stations such as WRP26, which are distant from the infiltration site, show relatively little change over the course of the infiltration events and confirm that background noise for this gravity monitoring is on the order of 10 μGal. Some far-field stations, including WRP05–07 and WRP 25, show larger variations (10–50 μGal) than typical regional background. These stations are either too far removed from the project site (1 km or more) to be influenced by the infiltrated water, separated from the site by stations showing smaller or no gravity changes and/or beyond likely no-flow boundaries (i.e., the Weber River). Furthermore, stations with greater noise and larger anomalies are close to drainage canals (WRP25) or the Weber River (WRP27) where leakage from these sources into the vadose zone is likely and would create a positive gravity anomaly. Accordingly, these local anomalies are likely because of other in-

fluences rather than the WRBASR infiltration (such as canal leakage or localized well pumping), and they reflect noise for the purpose of this study.

After the first period of infiltration, the gravity anomaly decreased gradually over time, from July 2004 until March 2005. The gravity anomaly at near-field stations declined by about half over the first three to four months. Over the next six months, gravity anomalies decrease further but remain at ~40 μGal above pre-infiltration background levels, suggesting that residual, perched infiltrated water remained near the site.

A second infiltration episode started on 17 March 2005, with an infiltration volume of 560,000 m^3 of water infiltrated over a two-month period. Infiltration was halted for three months because seepage occurred in the gravel pit. Once infiltration was resumed on 17 August, another 490,000 m^3 of water was recharged into the aquifer. Gravity values at stations near the infiltration ponds again responded quickly, with station WRP04 increasing by nearly 100 μGal from its value in early March 2005 to a total anomaly of 140 μGal after approximately five weeks. Station WRP01 yielded an even greater, but more erratic, anomaly and also stabilized at approximately 140 μGal. In both infiltration episodes, the response at station WRP27 is about 50% to 60% of the stations closer to the infiltration ponds. Note that measured gravity peaks during infiltration in 2005 are 40–50 μGal larger than the equivalent 2004 maximum values. The 40–50 μGal anomaly is likely the residual signal from the first infiltration event measured just before the second infiltration event started. Removal of this residual signal shows that both peaks have a magnitude of order 100 μGal. One might have expected a smaller gravity anomaly in the spring of 2005 because less water was infiltrated in the first 2005 episode than in 2004. However, the observation well, which had negligible response to the 2004 infiltration, recorded a 3-m rise during this period, so the gravity is responding to both infiltration above the silty layer and groundwater flow at the water table. After the second infiltration event, the gravity anomaly declines in a similar manner to the first event.

Evolution of the gravity field through the project is shown by a series of stick maps (Figure 5). The 4 March 2004 map (Figure 5a) depicts gravity prior to infiltration and shows negligible variation across the study area with all gravity anomalies less than 10 μGal. There is some evidence that the Weber River, which is a losing stream at the mouth of the canyon (Feth et al., 1966), might slightly affect gravity stations located close to the river. By 2 June 2004, two-thirds into the first infiltration event, the gravity anomaly is well developed and extremely localized (Figure 5b). Maximum gravity anomalies near the infiltration ponds are 110 μGal but far-field gravity is still near zero. Two weeks later (Figure 5c), the gravity anomaly has broadened, and stations farther from the site start to show significant increases. The decline of the gravity anomaly from its late June maximum to the fall of 2004 is illustrated in Figure 5d.

The second infiltration event in 2005 rejuvenates the gravity anomaly (Figure 5e). The 2005 anomalies appear larger, because of the residual signal from the 2004 event. The maximum anomaly in 2005 was approximately 190 μGal compared to the pre-infiltration values from 2004. The final map (Figure 5f) shows the decline of the rejuvenated mound and a suggestion of southward groundwater migration.

GPS data collection and results

Changes in gravity can reflect changes in either mass, elevation or both. With a free-air vertical-gravity gradient of −3.086 μGal/cm, small (3–5 cm) elevation changes can affect high-precision gravity data. Because valley elevations elsewhere along the Wasatch Front can change 2–5 cm seasonally (Merteens et al., 1998), precision GPS measurements were made every four to six weeks to monitor elevation changes at each station. We used two Trimble 4700 GPS receivers to acquire at least one hour of data at each station. Both GPS receivers were treated as rovers and compared to these continuous-GPS base stations: Eastern Ogden, Utah (EOUT), Strawberry/Snow Basin (SASU), and Northern Antelope Island, Utah (NAIU). GPS stations EOUT and NAIU are part of the UNAVCO network. Station SASU is maintained by the National Geodetic Survey (CORS).

GPS data were processed using Trimble Geomatics Office software in a post-processed, rapid-static mode. The GPS data indicated no significant (<2.5 cm) ground motion during the study, limiting gravity anomalies resulting from elevation changes to less than 8 μGal. Changes in gravity signal greater than 8 μGal can be attributed to infiltrated water and not elevation change. Because the GPS data analysis yielded no significant elevation changes, no further discussion of the GPS data is necessary and all models in this analysis assume that elevation changes are negligible.

DATA ANALYSIS AND APPLICATION

Having documented coherent and systematic gravity changes associated with aquifer recharge, now we focus on extracting additional information from results that relate the gravity data to hydrology. The nature of the resultant groundwater mound from the infiltrated water must be established first. We performed Gaussian integration of the spatial gravity anomaly to determine the anomalous mass in the subsurface and relate that to the volume and mass of infiltrated water. A minimum value for height of the groundwater mound (at its center) also can be estimated from the magnitude of the gravity anomaly by using a Bouguer slab approximation. The lateral extent of the groundwater mound is constrained by the edge of the gravity anomaly. Then hydraulic properties of the subsurface are derived from the transient decline of the gravity field, which is assumed to mimic the decay of the groundwater by flow through saturated porous media. The models used in this study assume that all gravity signals, after accounting for regional and seasonal effects and other measurement errors, represent signal from infiltrated mass.

The WRBASR project was conducted in an unsaturated area, with most mass change occurring in the vadose zone. However, we can interpret the results in terms of an effective groundwater mound, because the area of interest was rapidly saturated by the infiltrated water. In this study, it appears that the shallow vadose zone was saturated quickly, immediately above the low-permeability layer at 35 m below ground surface, forming a local perched aquifer. Details in timing and process as to how the locally perched mound proceeded to migrate through the clay layer and the underlying vadose zone to the water table (depth 70 m) are unclear. There was minimal change of water level in the observation well associated with the 2004 infiltration event. The water level was 71.02 m below the surface at the start of infiltration in March and rose gradually to 70.71 m by mid-May. It remained constant for the last half of the 2004 infiltration period. The 31-cm change could be entirely seasonal. Because the observation well was screened some distance below the silty layer and did not show any immediate response to infiltration, it is reasonable to assume that the silty layer impeded flow sufficiently to create a perched aquifer in 2004.

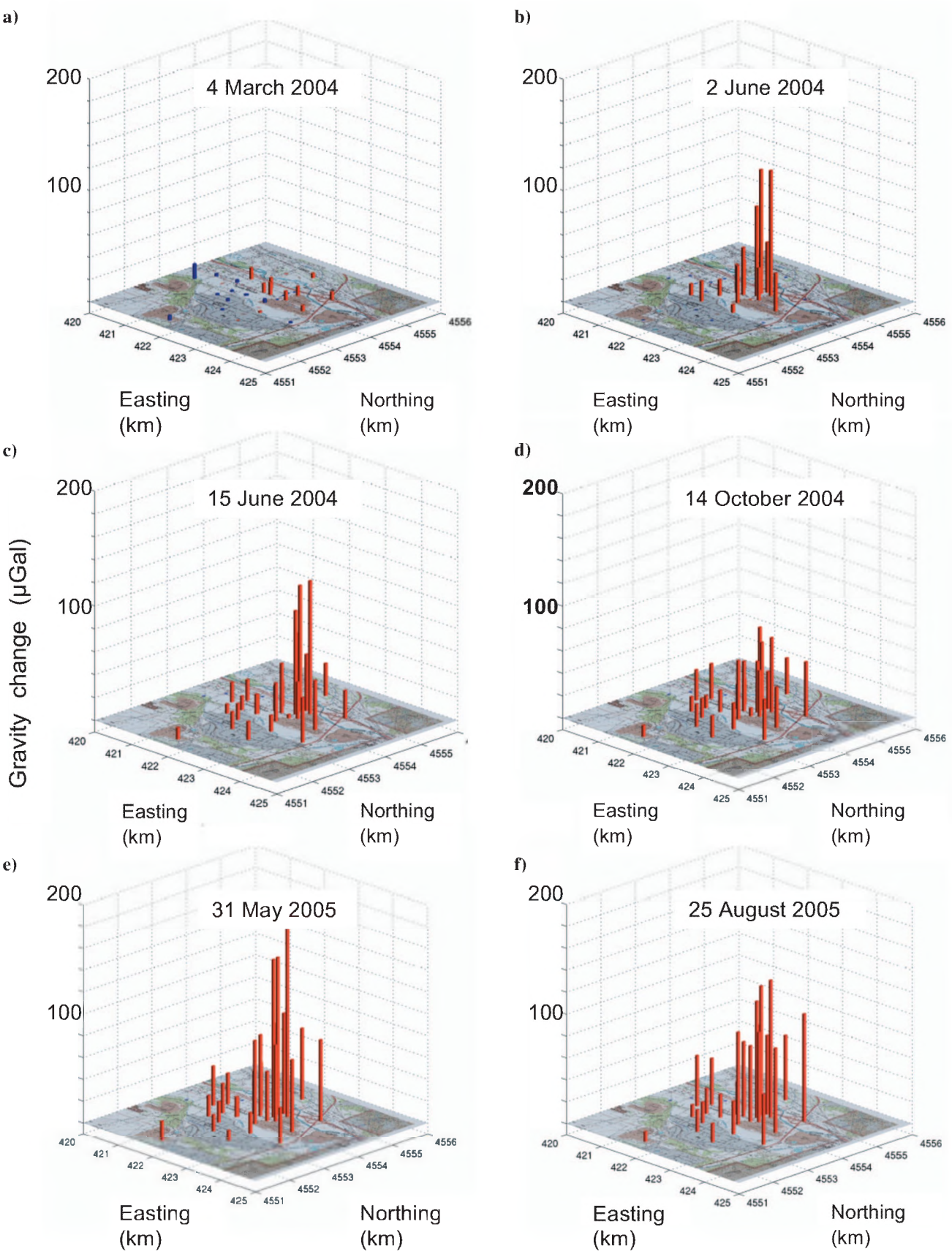

Figure 5. Stick maps showing evolution of the gravity anomaly throughout the study. The base map is from Figure 1. Dates of gravity surveys are given above each panel. Red represents positive gravity changes; blue represents negative changes.

Water levels in the observation well for the 2005 infiltration events are more complex. Still at 70.71 m at the start of infiltration on 17 March, the water level remained constant for a month but then rose by 3 m through 1 July, even though the infiltration was halted on 23 May because of seepage into the gravel pit. The level dropped slowly by 1.3 m through the end of August but regained a level of 67.9 m by the end of the 2005 infiltration on 31 October. The water level in the observation well has remained stable between 68 m and 66 m below the surface through two subsequent infiltration cycles in 2006 and 2007 when 1.4×10^6 m^3 and 1.6×10^6 m^3 of water, respectively, were recharged to the aquifers.

Gaussian integration and mass balance

The causative mass responsible for a confined gravity anomaly is calculated using Gauss's Theorem for potential fields observed over a plane (Telford et al., 1976). This theorem relates the magnitude (mass) of the causative body to the integral of the observed gravity anomaly at the surface

$$\int\int \Delta g(x,y)dxdy = 2\pi GM, \qquad (1)$$

where Δg is the measured change in gravity resulting from the excess mass, dx and dy are the spatial variables, M is the equivalent mass causing the gravity anomaly, and G is the universal gravity constant. Although the integral is over all space, we truncate integration at the edge of the gravity anomaly and integrate only over the nonzero region. Then the equivalent source mass M is calculated as follows:

$$M = \frac{\sum_{i=1}^{n}\sum_{j=1}^{m} \Delta g_{i,j} \cdot dx_i \cdot dy_j}{2\pi G} \qquad (2)$$

Figure 6, created from the June 30, 2004 survey at the end of the first infiltration event, shows the gridded gravity anomaly in a 3D projection that was used for a Gaussian integration. The inset shows the equivalent contour map of the gravity anomaly from the same survey. The contours are reasonably well constrained toward the peak of the anomaly, but there is considerable latitude in the contour configuration toward the edges of the anomaly. Gaussian integration of the observed gravity anomaly for this infiltration episode yielded a mass of $1.0 \pm 0.1 \times 10^9$ kg, the uncertainty arising from contouring, particularly placement of the zero-gravity anomaly contour. The calculated mass is very close to the actual mass obtained from the water budget from weir measurements. Figure 7 compares the weir-measured infiltrated mass to the mass calculated using Gaussian integration of the gravity anomaly after each campaign. The calculated mass generally mimics the actual infiltrated mass, although there are interesting discrepancies.

The uncertainty ($\pm 10\%$) in estimating the anomalous mass based on Gaussian integration of the gravity anomaly field arises in part from the difficulty of determining the exact zero boundaries of the gravity anomaly, and in part from the limited data (ten stations near the infiltration site). Furthermore, not all of the infiltrated mass remains detectable by our survey network. As water infiltrates deeper into the vadose and (eventually) saturated zones, it also spreads laterally, diminishing the change in the gravity signal. Also, infiltrated water flows eventually into the groundwater system beyond the boundary of detectable gravity change. These considerations explain why the gravity-calculated mass decreases by about 20% after infiltration stops, even though all of the mass is still in the subsurface. For the 2005 infiltration event, the increase in calculated mass again matches the increase for the infiltrated mass closely after incorporating the 20% offset.

Bouguer slab approximation

The magnitude of the gravity anomaly also can be used directly to constrain the spatial dimensions of a groundwater mound. The thickness of a broad groundwater mound can be related to the thickness of an infinite slab with a density contrast $\Delta\rho$ relative to unsaturated material by using the Bouguer infinite-slab approximation. This estimate is valid as long as the mound is close to the surface and has a sufficiently large radius. The mound with a top between 20 m and 25 m below the surface is assumed to form above the low-permeability silty layer, located ~35 m below ground surface. For this configuration, the Bouguer approximation is a fair estimate as long as the disc has a radius $\geq$200 m, approximately ten times the estimated depth to the top of the slab. From inspection of the gravity change maps in Figures 5 and 6, the groundwater mound should have a radius of at least 100–300 m. The change in density $\Delta\rho$ is determined by assuming that infiltrated water saturates the available pore space. The specific yield of the alluvial-fan material is estimated at approximately 0.2 for an effective porosity of 20%. Because the den-

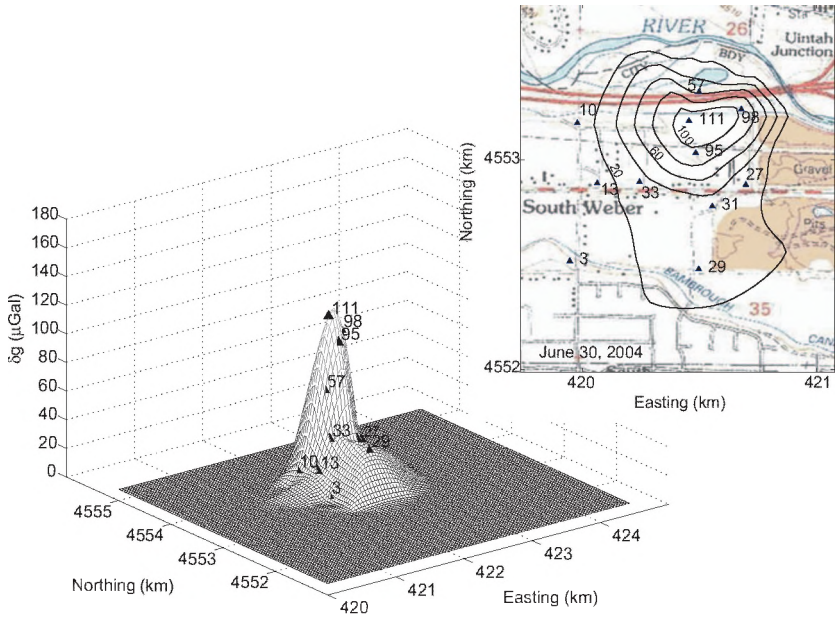

Figure 6. Gravity anomaly for the 30 June 2004 survey. Main image shows the gridded gravity anomaly used for Gaussian integration. The inset depicts the contoured gravity anomaly.

sity of water is 1000 kg/m^3, replacing the air in this pore space with water results in a $\Delta\rho$ of 200 kg/m^3. The thickness h of the groundwater mound at time t is given by

$$h(t) = \frac{\Delta g(t)}{2\pi \cdot G \cdot \Delta\rho}, \quad (3)$$

where $\Delta\rho$ is the change in density from presaturated to saturated aquifer media, Δg is the measured change in gravity at time t, and G is the universal gravity constant.

The maximum gravity anomaly, measured at the end of infiltration, was 111 μGal, equating to a mound thickness of ~13.5 m for an effective porosity of 20%. For a mound thickness of 13.5 m in a medium with 20% effective porosity, the volume of a cylindrical disc that would contain the 10^6 m^3 of water in the pore space requires a radius of ~345 m.

Spatial gravity anomaly and groundwater mound geometry

Another method for constraining the radius of the groundwater mound equates the gravity effect computed for groundwater mounds of various radii to the observed spatial gravity anomaly. Measured gravity as a function of radial distance from the infiltration site (station WRP04) is compared to computed gravity profiles for subsurface discs, representing different groundwater-mound geometries. Groundwater mounds are represented as buried discs with height h, radius r, and density contrast $\Delta\rho$, with the top of the disc at a specified depth beneath the surface. The computed gravity field of the disc is compared to the measured gravity-field profile to find a radius of the groundwater mound that matches the observed data most closely. Figure 8 shows the gravity data and the profiles for various values of disc radius. This model uses an effective porosity of 20% and assumes that the bottom of the groundwater mound formed at the silty layer (35 m depth). For a mound height of 13.5 m, the top of the mound would be 21.5 m below the surface.

The modeling results indicate that a groundwater mound 13.5 m high with a radius of 300–400 m best fits the measured gravity changes with distance. This estimate is close to the radius derived using the Bouguer slab approximation and water-mass balance (345 m). The evolution of the gravity field exhibits some asymmetry, suggesting a groundwater flow to the south-southwest and hence departing from a perfect cylindrical shape for the recharge mound. Thus some discrepancy is expected when comparing a buried disc with the measured gravity data. Nonetheless the comparison yields another reasonable estimate of mound radius, which in turn provides another estimate for the effective hydraulic conductivity of the aquifer.

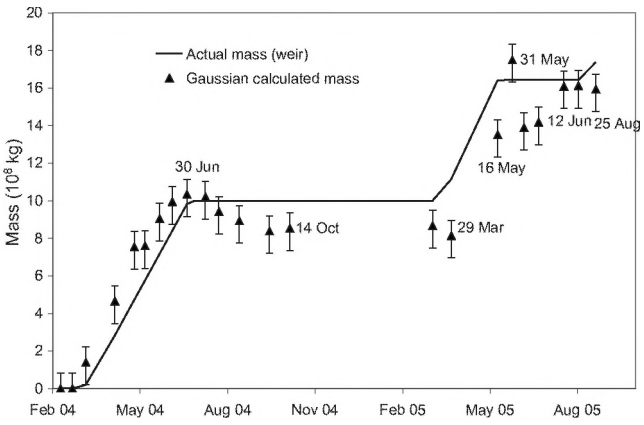

Figure 7. The mass of infiltrated water measured at weir (solid line) compared with the mass estimated from Gaussian integration of the gravity anomalies.

Groundwater mound decay and hydraulic conductivity

Groundwater flow properties can be inferred by relating the decline of the measured gravity signal to the modeled decay of the height of an underlying groundwater mound. We assume that any decrease in the measured gravity anomaly is correlated directly to a decrease in the thickness of the groundwater mound (see equation 3). The goal is to relate gravity changes to the hydraulic conductivity of the subsurface.

Decay of an axially symmetric groundwater mound with time can be expressed (Bear, 1988) by

$$h(r,t) = \frac{h_o}{\left(1 + \frac{8Kh_o}{\Phi_e r_o^2} t\right)} \left[\left(1 + \frac{8Kh_o}{\Phi_e r_o^2} t\right)^{1/2} - \left(\frac{r}{r_o}\right)^2 \right] \quad (4)$$

where $h(r,t)$ is the height of the mound at distance r from the center of the mound at time t, h_o is the initial height at $r = 0$ and $t = 0$, K is the hydraulic conductivity of the medium, Φ_e is the effective porosity of the medium, and r_o is the initial radius of the groundwater mound. In this case, we are interested in the change in the height at $r = 0$ (the center of the mound) over time. We assume effective porosity for this alluvial medium to be 20%. This equation assumes a constant hydraulic conductivity, saturated conditions for the mound, and that laterally adjacent regions become saturated as the mound spreads. Thus for this comparison, we assume that the volume con-

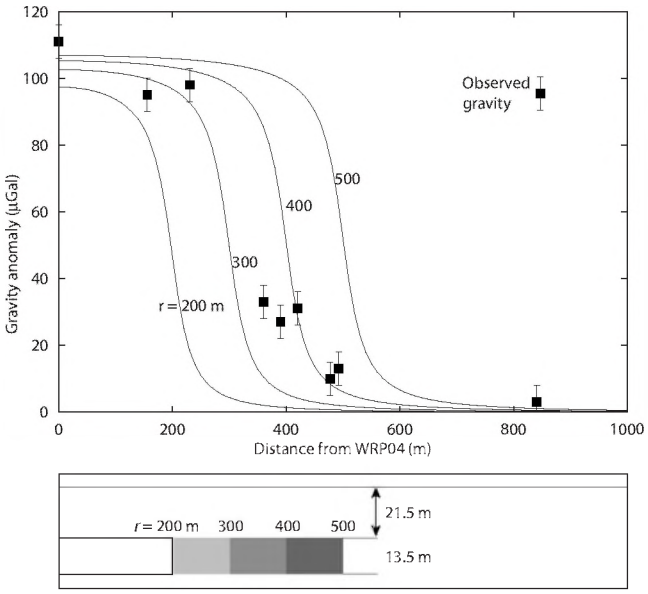

Figure 8. Gravity anomaly and model results for a buried horizontal disc. Disc radii are varied from 200–500 m. Observations for the 30 June 2004 survey are plotted with respect to radial distance from WRP04.

sisting of the mound is saturated and flow occurs as the mound spreads laterally by saturating the adjacent pore space. In this manner, saturated hydraulic conductivity of the alluvial material is estimated. Inaccuracy in assumptions for this formulation of a groundwater-mound decay will, of course, lead to errors in the parameters determined.

Figure 9 shows the change in gravity at station WRP04 over time after infiltration ended on 2 July 2004, normalized to its initial maximum value of 111 μGal. The gravity anomaly decreases rapidly at first and then more slowly; it decreases to 50% of its initial value in about 3.5 months, and to 40% of its original value after approximately seven months. Figure 9 also depicts the normalized decay of the groundwater mound computed from equation 4, using an initial mound radius of 350 m. Note that these decay curves are independent of mound height. Different curves represent an array of hydraulic conductivities ranging from 5 to 120 m/day. For this mound radius, the gravity data are exceptionally well fit by a hydraulic conductivity of 80 m/day. However, if the mound radius is increased, then the best fit for hydraulic conductivity is larger because it requires a more conductive media to draw down a relatively wider and flatter groundwater mound.

The results of modeling groundwater-mound decay for a variety of mound radii are illustrated in Figure 10. The figure also shows a range of effective porosities (shaded area) from 0.1 to 0.3; the center line represents the preferred effective porosity used in this paper (0.2). The groundwater-mound radius was varied in increments of 50 m; for each specified radius, a minimization process determined the optimum hydraulic conductivity. Without knowledge about the groundwater-mound radius, the hydraulic conductivity which best explains the mound decay is bounded absolutely between 5 m/day for a mound radius of 100 m and 100 m/day or even higher for a mound radius of 400 m. However, the groundwater-mound radius can be bounded in several ways. We provide minimum bounds by finding the radius of a circle that (1) has the same area of the four infiltration ponds, or (2) encloses all of the ponds (Figure 3); those radii are 69 m and 110 m, respectively. It is unlikely the mound is that small, however, because the infiltrated water has three months to spread prior to infiltration stopping. Recall that the estimate for mound radius was 345 m from the water budget and Bouguer slab approximation, and 300–400 m obtained by modeling the spatial configuration of the full gravity anomaly (Figure 8). The best-fitting hydraulic conductivities for these three radii (300 m, 345 m, and 400 m) are 60 m/day, 75 m/day, and 100 m/day, respectively, using an effective porosity of 0.2.

Our preferred hydraulic conductivity of 80 m/day from gravity monitoring falls neatly within the textbook ranges reported for unconsolidated materials (Table 4.3 in Schwartz and Zhang, 2003). Hydraulic conductivity for sands ranges from 4 m/day (fine sand, poorly sorted) to 57 m/day (very coarse sand, well sorted). Gravel conductivities appropriate for the Weber Delta aquifers vary from 49 m/day (fine gravel, poorly sorted) to 143 m/day (medium-to-coarse gravel with moderate sorting). By comparing the decline of the gravity signal with this groundwater-decay model, we have determined an estimate of hydraulic conductivity on the 100–500 m scale. Such a scale length is normally difficult to achieve. Laboratory measurements are obtained on a sample scale of 10 cm. Aquifer tests provide accurate conductivities at the tens of meters scale, but they also require costly well installation and pump tests, which are not always feasible. The scale sensed by the recharge pilot project and 4D gravity is appropriate for the alluvial-fan material composed of interfingering gravels and sands.

DISCUSSION

Gravity monitoring at the WRBASR project shows that 4D gravity captured the growth, peak, and decay of the infiltrated mass over time for two recharge events spaced a year apart. It also tracked area groundwater flow in a general sense. The gravity data indicate southward flow, supporting the existence of a low-permeability layer with a southward dip or some anisotropy in hydraulic properties of the alluvial material.

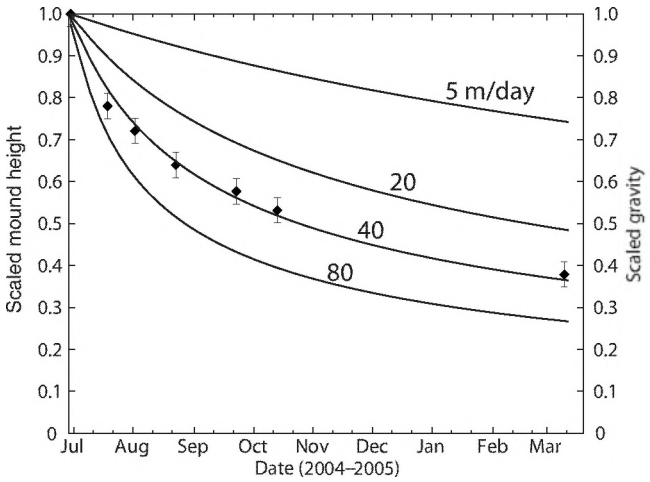

Figure 9. Groundwater-mound decay compared with measured gravity. Solid lines show decay of the groundwater mound with radius of 350 m for various values of hydraulic conductivity calculated using equation 4. Gravity-anomaly data (solid symbols) are for WRP04, normalized to the value on 30 June 2004.

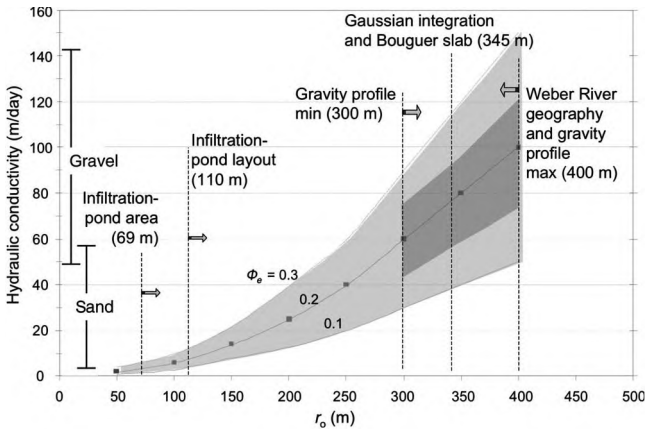

Figure 10. Constraints on hydraulic conductivity of the alluvial fan. Curves show optimum hydraulic conductivity required to match the decay of the gravity anomaly with the decay of a groundwater mound for a range of mound radii. Vertical lines indicate constraints on the mound radius discussed in text. The dark gray region shows the most likely parameter space for a porosity range of 0.15 to 0.25, centered on a porosity of 0.20, and a mound radius from 300–400 m. The preferred hydraulic conductivity is 80 m/day.

Although the focus of this study was on the near-field region of the infiltration ponds, some far stations did show above background-gravity readings, which must be addressed. Sites WRP05 and WRP07 are north of the Weber River and beyond reasonable distance for infiltrated water to travel. However, these sites show positive gravity anomalies during infiltration between 15 μGal and 52 μGal. It is unlikely that infiltrated water would undercut the river and migrate more than 1 km to the north (against the general groundwater-flow direction). It is more likely that these stations are recording a strong, localized natural signal or some other anthropogenic influence. For example, these stations are located near a nursery and might represent fluxes because of seasonal irrigating and pumping. Also, WRP06, WRP07, WRP25, and WRP27 are close to the Weber River and/or irrigation canals, which are known to leak and could cause the larger observed gravity anomalies at these sites.

Other sites to the east (WRP08 and WRP25) also show moderate gravity signals of 20–30 μGal during the study period. These stations could be influenced by infiltration potentially, except that stations located between WRP08 and WRP25 and the project site (i.e., WRP02) show a lesser gravity response, indicating that the signal farther to the east does not result from the aquifer-recharge infiltration. There are several irrigation ditches near these eastern stations. Although they are lined to reduce water loss, fractures in the lining and heavy vegetation along the ditches indicate that water is leaking from the ditches. In addition, these sites might be capturing natural runoff from the eastern adjacent hills. Furthermore, these eastern stations are situated close to the mouth of the canyon and therefore are higher in elevation. It is not likely that infiltrated water would flow that far uphill, against topography and the regional gradient.

Mass calculations derived from Gaussian integration during early gravity campaigns match the infiltrated mass to within 20%. After June 2004, calculated mass decreases as the mound infiltrates away from the study site and the gravity signal decreases. Data from the 2005 infiltration events show a similar trend in which the calculated mass is within 20% of the actual mass until infiltration stops and the gravity signal begins to decrease. This deficiency in the mass after infiltration stops can have several causes. Over time, some of the mass has infiltrated deeper and away from near-field stations, resulting in a reduced signal at these stations. In an ideal system, all of the signal would be captured by stations farther from the infiltration site. However, because of the limited number of gravity stations and background noise of approximately 10 μGal, the broader, reduced signal from the deeper mass was not distinguishable or captured completely.

In addition, the mass deficiency might partially be an artifact resulting from gridding the scattered gravity data set. The sparse nature of our monitoring network, particularly to the north and east of the site, makes it difficult to define the anomaly boundaries accurately. We have chosen to minimize the anomaly area, using the Gaussian integration results as a lower bound as the water flows away from the surface and study area. In the future, researchers should consider installing more gravity stations near the infiltration site for surveys of this kind, with additional stations located at 500 m and 750 m from the site. Such a configuration would give more confidence in capturing the localized peak and gradual spread of the subsurface water, and provide a more accurate boundary for the gravity anomaly. In addition, more data points would increase the accuracy and confidence in Gaussian integration and mass-calculation techniques.

Sites with no laterally extensive clay or silty layers would provide the most efficient setting for future aquifer-recharge efforts. In sites like the Weber Delta, injection wells could be installed to ensure that infiltration occurs below low-permeability layers. Injection wells screened below 35 m would bypass the clay layer, while still allowing passive (gravity-driven) infiltration to recharge the aquifer. Such a geometry would reduce horizontal flow and minimize residual water in the vadose zone. In addition, the reduced lateral flow would facilitate high-precision gravity surveys by allowing for a tighter, smaller station grid.

CONCLUSION

Repeated high-precision gravity surveys were made over two annual infiltration cycles on an alluvial fan at the mouth of Weber Canyon, northern Utah, as part of the Weber River Basin Aquifer Storage and Recovery Pilot Project (WRBASR). Gravity data collected before, during, and after infiltration events provides evidence that a groundwater mound formed during the infiltration events and that the mound decayed smoothly with a gradual migration south-southwest of the infiltration ponds. This study also shows that high-precision gravity data can be used to establish reasonable bounds for hydraulic properties of the underlying aquifer and unconsolidated sediments in the alluvial fan.

Observations and modeling of the 4D gravity field permit the following observations and conclusions:

1) Scintrex reports the precision of the CG-3M gravimeter used in this study to be 1 μGal. Instrument drift, natural signal variation and noise in the gravity monitoring project indicate a practical detection limit of 10 μGal. The signal from groundwater infiltration in the near-field ranges from 40 to 194 μGal and therefore is well above detection limits. Any similar project in 4D gravity could be monitored with a similar instrument as long as the expected signal is at least 20–30 μGal above natural background variation. For future survey design purposes, we note that saturating a subsurface layer of 1 m with an effective porosity of 0.2 produces a gravity change of 8.4 μGal.
2) Maximum measured gravity changes at WRP04 (nearest the infiltration site) associated with the recharge events of the WRBASR project were 110 μGal during the first event (2004) and an increment of approximately 130 μGal during the second event (2005).
3) An array of 30 gravity stations was sufficient to track the growth, decline, and migration of the gravity anomaly caused by a mounded water table and migration of infiltrated groundwater. The project would have benefited from more stations close to the infiltration ponds and fewer far-field stations.
4) Gaussian integration of the spatial gravity anomaly yielded an anomalous, localized mass almost identical to the 1.0 kg $\times 10^9$ kg associated with the 2004 infiltration event. Mass calculated from the gravity data throughout infiltration remained within 10–20% of the infiltrated mass. Greater accuracy could be achieved with additional stations near the infiltration site to delineate better the zero-gravity anomaly boundary.
5) Three-dimensional gravity modeling of a shallow disc implies that the groundwater mound at the cessation of the three-month infiltration period in 2004 had a thickness of 13.5 m and a radius of 300–400 m. This mound thickness is also consistent with a Bouguer slab approximation to determine mound thickness and the water budget to obtain a disc radius.

6) After infiltration was stopped, the gravity anomalies decreased to about 50% of the original amplitude over a characteristic time of three to four months. The decline is simulated extremely well by analytical solutions for the decay of a groundwater mound by flow through saturated porous media. Modeling the decay places tight bounds on the hydraulic conductivity of the alluvial fan below the recharge site if the original radius of the mound is known. The preferred hydraulic conductivity, assuming a groundwater-mound radius of 350 m in a medium with 20% effective porosity is 80 m/day with reasonable bounds of 60–100 m/day. These values represent the conductivity of the alluvial fan at a scale length of hundreds of meters.

This study shows that high-precision gravity surveys provide a relatively cheap, efficient, and accurate technique for tracking water recharge and movement in the shallow subsurface in areas with few groundwater monitoring wells or where well installation is cost prohibitive. It would be ideal to couple continuous measurements at a key site (e.g., WRP04 in our study) with repeat surveys at many stations over the area of interest. A detailed groundwater model with more field-based parameters would be another ideal complement to gravity monitoring. An area with well-documented lithology, in situ piezometers, and groundwater-monitoring wells would provide an ideal setting to test further the detection limits and accuracy of high-precision 4D gravity.

ACKNOWLEDGMENTS

The authors thank Hugh Harlow and Mike Lowe of the Utah Geological Survey for logistical assistance and support. Rick Allis, Rob Harris, and Michael Thorne read the manuscript and made helpful suggestions.

REFERENCES

Allis, R., and T. Hunt, 1986, Analysis of exploitation-induced gravity changes at the Wairakei Geothermal Field: Geophysics, **51**, 1647–1660.

Anderson, P. B., D. D. Susong, S. R. Wold, V. M. Heilweil, and R. L. Baskin, 1994, Hydrogeology of recharge areas and water quality of the principal aquifers along the Wasatch Front and adjacent areas, Utah: U. S. Geological Survey, Water Resources Investigations Report 93-4221.

Bear, J., 1988, Dynamics of fluids in porous media: Courier Dover Publications.

Bonvalot, S., M. Diament, and G. Gabalda, 1998, Continuous gravity recording with Scintrex CG-3M meters: A promising tool for monitoring active zones: Geophysical Journal International, **135**, 470–494.

Budetta, G., and D. Carbone, 1997, Potential application of the Scintrex CG-3M gravimeter for monitoring volcanic activity: Results of field trails on Mt. Etna, Sicily: Journal of Volcanology and Geothermal Research, **76**, 199–214.

Clark, D. W., C. L. Appel, P. M. Lambert, and R. L. Puryear, 1990, Groundwater resources and simulated effects of withdrawals in the east shore of Great Salt Lake, Utah: Utah Department of Natural Resources, Technical Publication 93.

Clyde, C. G., C. J. Duffy, E. P. Fisk, D. H. Hoggan, and D. E. Hansen, 1984, Management of groundwater recharge areas in the mouth of Weber Canyon: Utah Research Laboratory, Hydraulics and Hydrology Series UWRL/H-84/01.

Dragert, H., A. Lambert, and J. Liard, 1981, Repeated precise gravity measurements on Vancouver Island, British Columbia: Journal of Geophysical Research, **86**, 6091–6106.

Ferguson, J. F., T. Chen, J. Brady, C. L. V. Aiken, and J. Seibert, 2007, The 4D microgravity method for waterflood surveillance II: Gravity measurements for the Prudhoe Bay reservoir, Alaska: Geophysics, **72**, no. 2, I33–I43.

Feth, J., D. Barker, L. Moore, R. Brown, and C. Veirs, 1966, Lake Bonneville: Geology and hydrology of the Weber delta district, including Ogden, Utah: U. S. Geological Survey, Professional Paper 518.

Gates, J. S., 1995, Description and quantification of the ground-water basins of the Wasatch Front, Utah: in W. R. Lund, ed., Environmental and engineering geology of the Wasatch Front region: Utah Geological Association, Publication 24.

Gettings, P., 2005, Repeated high-precision gravity surveys in the Salt Lake Valley, Utah: M. S. thesis, University of Utah.

Gettings, P., D. S. Chapman, and R. Allis, 2008, Techniques, analysis, and noise in a Salt Lake Valley 4D gravity experiment: Geophysics, this issue.

Hurlow, H., M. Lowe, and M. Matyjasik, 2008, The Weber River Basin aquifer storage and recovery pilot project: Utah Geological Survey, contract report to Weber Basin Water Conservancy District.

Jachens, R., D. Spydell, G. Pitts, D. Dzurisin, and C. Roberts, 1981, Temporal gravity variations at Mount St. Helens, March-May 1980: U. S. Geological Survey, Professional Paper Report P1250, 175–181.

Keysers, C. J., H. J. Kuempel, and J. Campbell, 2001, Local seasonal gravity changes in the Lower Rhine Embayment, Germany: Acta Geodaetica et Geophysica Hungarica, 36, 313–326.

Lowe, M., H. Hurlow, and M. Matyjasik, 2003, The Weber River Basin aquifer storage and recovery project: Utah Geological Survey, Open-file report 419.

Merteens, C., R. Smith, W. Chang, C. Puskas, and T. V. Hove, 1998, GPS-determined deformation of the western U. S. Cordillera, Wasatch Front, Utah, and Yellowstone: EOS Transactions of the American Geophysical Union, **79**, no. 45, F203.

Pool, D., and J. Eychaner, 1995, Measurements of aquifer storage change and specific yield using gravity surveys: Ground Water, **33**, 425–432.

Pyne, R. D. G., 1995, Groundwater recharge and wells: A guide to aquifer storage and recovery: Lewis Publishers.

Schwartz, F. W., and H. Zhang, 2003, Fundamentals of groundwater: John Wiley and Sons.

Stonely, T., 2004, Weber River Basin: Planning for the future: Utah Division of Water Resources, Comprehensive Water Planning.

Tamura, Y., 1987, A harmonic development of the tide-generating potential: Bulletins d'Informations Marées Terrestres, **99**, 6831–6855.

Telford, W. M., L. P. Geldart, R. E. Sheriff, and D. A. Keys, 1976, Applied geophysics: Cambridge University Press.

Whitcomb, J. H., W. O. Franzen, J. W. Given, J. C. Pechman, and L. J. Ruff, 1980, Time-dependent gravity in southern California, May 1974 to April 1979: Journal of Geophysical Research, **85**, 4363–4373.